The failure mechanism of field polyethylene gas pipeline with gas leakage at electrofusion joint

Qing Bao and Baojin Wang
The Fourth Subsidiary, Beijing Gas Group Co Ltd, Beijing, China

Manman Li
Beijing Gas Group Co Ltd Research Institute, Beijing, China, and

Chao Li, Chao Li and Jin Gao
Institute for Advanced Materials and Technology, University of Science and Technology Beijing, Beijing, China

Abstract

Purpose – A section of in-service PE gas pipeline in Guocun, Beijing, was found to appear gas leaking at the electrofusion (EF) joint. This study is dedicated to reveal the material cause of EF joint failure to help with a more accurate prediction of service life of PE gas pipe and further normalize the construction of PE gas pipeline.

Design/methodology/approach – Defect detection was carried out on the leaking EF joint using ultrasonic phased array. The mechanical degradation and structural aging behavior was studied by tension test, FTIR technology, TG test and DSC test. The organic components in the soil surrounding the PE gas pipe failure area were qualitatively identified.

Findings – The results showed that the organic surfactants in the soil environment could accelerate the aging behavior of PE material, leading to a deterioration of mechanical properties and a serious reduction in the ability of the PE pipe and EF joint, especially at the welding defect, to resist external force.

Originality/value – A novel study was conducted to investigate the failure cause of the EF joint of in-service PE gas pipe, incorporating the analysis of environmental factors and structural deterioration.

Keywords Electrofusion joint, Polyethylene gas pipe, Failure analysis, Surfactants, Aging

Paper type Research paper

1. Introduction

PE gas pipelines are often buried underground and require long-term service, so the mechanical properties of polyethylene (PE) gas pipelines are strictly required. In accordance with the standard CJJ 63–2018, which mandates a service life of PE gas pipe for 50 years, it is imperative to accurately assess the safety performance and lifespan of these components. According to the Plastic Piping Data Collection (PPDC) statistics on the failure locations of PE pipes in the USA, 69.7% of the pipe failures occur at the pipe fittings and joints. The electrofusion (EF) joint is regarded as the weakness of the piping system and has drawn huge focus in the quality control of PE pipe network (Leskovics *et al.*, 2006; Shapheek and Shrivastava, 2020). However, the defect inspection methods for EF joints are quite limited, unlike those for hot fusion joints, which can undergo further detection through flanging excision inspection. Welding quality control in the construction of EF joints generally relies on process control and appearance inspection. This process is subjective and cannot observe the internal defects of the welded joints, which are gradually exposed with the service time of the PE gas pipeline, bringing serious safety hazards. Phased array ultrasonic testing (PA-UT) is the most feasible way to detect the defects in EF joint and to further explore the reason for improvement (Matthew *et al.*, 2016; Egerton *et al.*, 2017). Caravaca *et al.* (2007) found that the ultrasonic phased array inspection performed consistently in cold fusion and surface contamination detection. The extrusion peeling test showed that the ultrasonic phased array technology is reliable in detecting the quality of PE EF welding.

PE gas pipes are subject to various factors during field service, including environmental factors (temperature/humidity, surfactant, impact of internal pressure and external forces) and pipe structure, which severely limits their service life. These factors significantly constrain their service life. Extensive research has centered on examining the thermo-oxidative aging behavior of PE gas pipes, aiming to assess their performance and predict their service life (Weon, 2010; Mei, 2004; Wang *et al.*, 2000; Li and Chen, 1998; Zha *et al.*, 2023; Grabmayer *et al.*, 2014; Chen *et al.*, 2019; Wang *et al.*, 2019). For example, Weon's (2010) study revealed that during the initial stages of aging, the enhancement in crystallinity and tensile strength of linear low-density PE (LLDPE) pipes, along with the formation of carbonyl groups, indicated the onset of degradation. Hoàng and Lowe (2008) investigated the

oxidation consumption pattern of blue PE pipes during static hydraulic processes, observing a reduction in the oxidation induction period and the presence of hydrogen peroxide. Li et al. (2019) examined the variations in the thermal stability of PE gas pipes throughout the aging process. Similarly, Wang and Peng (2005) analyzed the structural and mechanical alterations in high-density PE (HDPE) pipes after exposure to natural conditions in Hainan and artificial aging using a xenon lamp.

Beyond thermo-oxidative aging, the potential for aging failure induced by chemical media merits significant attention (Zha et al., 2022). Zha et al. (2023) reported noticeable aging in PE pipes that had been operational for 15 and 25 years, albeit exhibiting less aging than those subjected to 10,000 h of artificial aging. Xiong et al. (2011, 2016) developed a composite surfactant solution that exhibited a more pronounced acceleration effect in evaluating the slow crack growth performance of HDPE pipes compared to a nonylphenol polyoxyethylene ether surfactant solution. This advancement facilitates the accelerated development of HDPE pipes. It is evident that surfactants in the operational environment significantly influence the aging behavior of PE pipes, as observed by Bredács et al. (2018). Consequently, relying solely on individual artificial aging methods for failure analysis of PE pipes is inadequate. Nevertheless, there remains a gap in understanding the specific soil characteristics encountered in the field and their impact on the in-service performance of PE pipes.

In this article, the structural causes of the failure of EF joints and PE pipes near the gas leak point have been analyzed through mechanical testing and material structure aging analysis. Additionally, ultrasonic phased array technology was used to detect defects in the EF joints. Chemical substances present in the soil samples collected near the leak point were also tested. Finally, combining these results, the acceleration mechanism of surfactants on the aging of PE pipe materials is elucidated. These insights are crucial for understanding the aging process of buried PE gas pipes and assessing their long-term serviceability, thus laying a solid foundation for the effective management and construction of PE gas pipe networks.

2. Experiment

2.1 Sample preparation

In 2022, a gas leak incident transpired in Guocun Village, located within Yujiawu Township in Tongzhou District. The leak emerged at the EF joint after five years of service. The soil surrounding the leak site, at a depth of 0.8 m, was characterized as dry, coarse and sandy. The root cause of the gas leak was traced to the height discrepancy between the branch pipe and the main pipe, which induced excessive bending stress on the EF joint, ultimately leading to the exposure of the heating wire. Figure 1 depicts the emergency repair construction site and pinpoints the precise location of the leak. The compromised EF joint and the PE pipe (P1) were retrieved for subsequent laboratory analysis. It is worth noting that the pristine pipe (P2) shares the same material composition and manufacturing process as the pipe that was in service.

Figure 1 The emergency repair construction site and gas leakage location

DE110/Low voltage
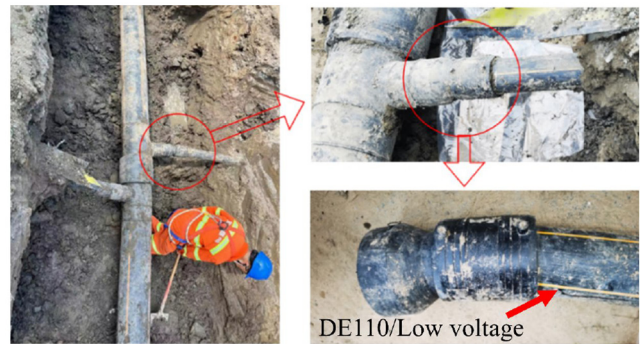
Source: Authors' own creation

2.2 Ultrasonic phased array

To study the impact of the soil environment on buried PE pipes, the Phascan II 32/128PR ultrasonic detector produced by Doppler Electronic Technologies Co., Ltd. was used to detect defects in the EF joint. This advanced instrument used B-scan real-time imaging technology and uses a 7.5 MHz probe for accurate detection.

2.3 Physical and chemical analysis of soil samples

To gain a profound understanding of the soil environment's impact on buried PE pipes, a rigorous analysis was conducted on the organic components surrounding the failure area of the PE gas pipe. Adhering to the HJ834-2017 and HJ605-2011 guidelines, semi-volatile and volatile organic compounds were extracted from the soil. These organic compounds' peak/spectrum was then precisely measured using a Trace/1300 ISQ QD gas chromatography-mass spectrometer. By comparing the obtained spectra with a comprehensive organic compound spectrum library, the diverse organic compounds present in the soil were qualitatively identified. Additionally, the microscopic morphology of the failed PE pipe's outer surface was examined using a JEOL JSM 6700F scanning electron microscope (SEM), providing further insights into the pipe's degradation.

2.4 Tensile test

To ensure accurate and consistent results, the tensile test sample is carefully prepared according to the requirements of GB/T 8804.3-2003. The sample is of type I dumbbell shape. Tensile test was employed on a microcomputer-controlled electronic universal testing machine in the speed of 200 mm/min. The break elongation I_e is obtained according to equation (1):

$$I_e = \frac{L - L_0}{L_0} \times 100\% \qquad (1)$$

where L_0 is the initial gauge length, and L denotes the gauge length after fracture.

2.5 Fourier transform infrared spectroscopy analysis

FTIR (Nicolet FTIR, 6700, Thermo Fisher Scientific) was tested on P1 and P2 pipes with a total reflection infrared spectrometer. The testing range was 350–4,000 cm^{-1}.

The reflective crystal was ZnSe, The incident angle was set at 45°, and the scanning time was 32 times with the resolution of $0.35 \, \text{cm}^{-1}$.

2.6 Thermogravimetric analysis

According to GB/T 33047.1–2016, a thermogravimetric (TGA) analyzer (Q5000IR, TA Instruments) was used to conduct TGA tests on P1 and P2 pipes. The sample weight was 10–15 mg. All samples were heated from room temperature to 550°C at a heating rate of 10°C/min under a nitrogen atmosphere. The initial and final masses of the samples were recorded, and the percentage weight loss as a function of temperature was measured using the TGA analysis program.

2.7 Melting temperature and crystallinity test

According to GB/T19466.1-2004, the differential scanning calorimeter (60Aplus, Shimadzu Corporation, Japan) was used to determine the non-isothermal crystallization behavior of PE pipes. The DSC test was performed in the temperature range from 25°C to 170°C, with a heating rate of 20°C/min. Samples were placed in nitrogen atmosphere with a gas flow rate of 50 mL/min. The melting temperature (T_{eim}), melting peak temperature (T_{pm}) and the melting enthalpy (ΔH) are obtained from DSC curves. The crystallinity (X_c) is calculated based on equation (2):

$$X_C = \Delta H / \Delta H_{100} \qquad (2)$$

where ΔH_{100} represents the melting enthalpy (J/g) of the target sample when the crystallinity is 100%, and its empirical value is 293 J/g.

2.8 Oxidation induction time test

According to GBT 19466.6-2009, the oxidation induction time (OIT) test was conducted on PE pipes using TA2910 DSC instrument. The test involved maintaining air and N2 gas flow rates at 100 cm³/min, initiating ventilation at 15 min for P1 and 16 min for P2 and maintaining a test temperature of 210°C.

3. Results and discussion

3.1 Ultrasonic phased array detection

As a nondestructive testing method, ultrasonic phased array detection (UPAD) can focus the welding area of PE pipe in all directions and demonstrate the structural flaws (Tao *et al.*, 2023). UPAD technology is easy to operate, and it can detect several defects and different defects have obvious defect characteristics in the UPAD map (Li *et al.*, 2023). EF joint has four typical defects in such as wire dislocation, hole, lack of fusion and cold fusion (Zheng *et al.*, 2012). The UPAD results of the leaking EF joint, obtained from the emergency repair site, are presented in Figure 2.

In Figure 2(a), a normal EF joint is characterized in well-organized resistance wires without any notable dislocations in the ultrasound image. The characteristic line above the heat wires is in right place. The inner wall of the EF fittings integrates seamlessly with the pipe material, and a fusion line is visible on the image. This fusion line is situated at a set distance

Figure 2 Phased array mapping, (a) normal EF joints; (b)–(c) failed EF joints
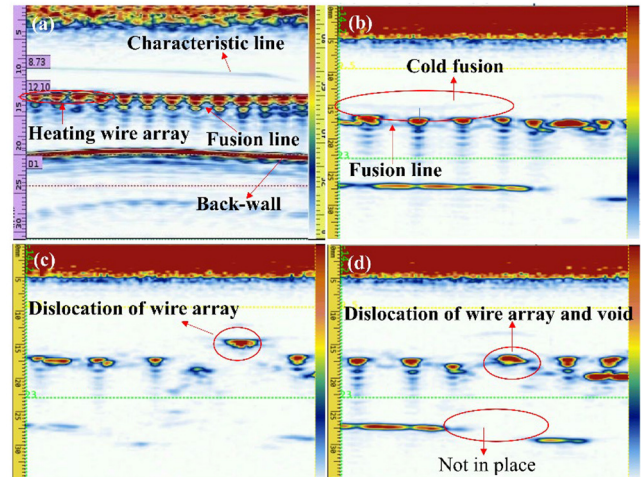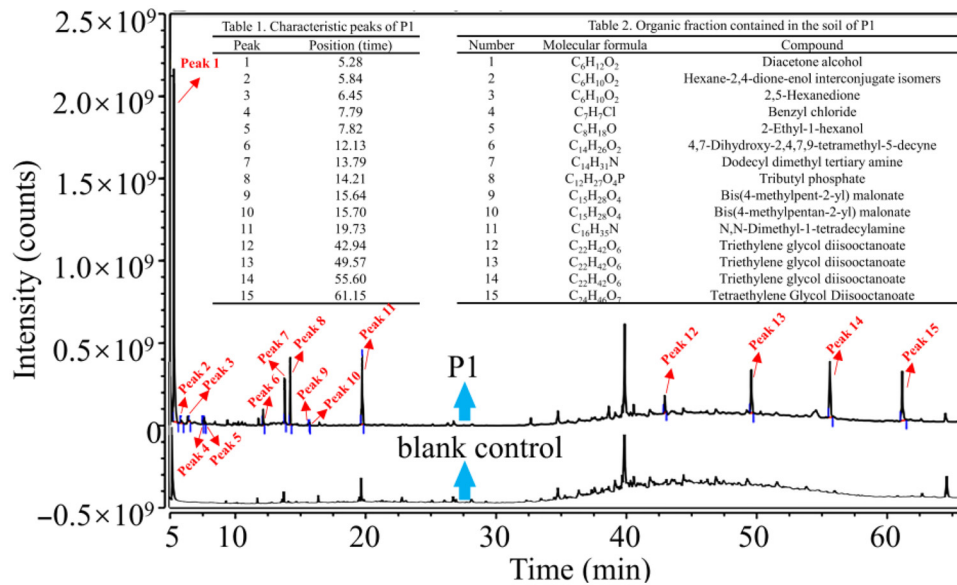

Source: Authors' own creation

below the heat wire and runs parallel to the back-wall. Due to interference from the wire signal, fusion line can be seen as a connection line between different wire signals. Apart from the wire signal, there are no notable brightening, thickening or disappearance phenomena. The inner wall of the pipe displays a continuous and clear signal, and there are no other obvious signals in the welding area (Shin *et al.*, 2003).

In Figure 2(b), the distance between the characteristic line (the boundary between the molten and unmolten areas of the pipe or pipe fitting, marked by a red circle) and the wire is shorter than the standard, indicating a cold fusion in EF joint (Frederick *et al.*, 2010). According to DB 31/T1058-2017 standard, the cold fusion degree H is 48%. In Figure 2(c), the heating wire distribution appears uneven due to displacement during the welding process. Typically, over-welding is accompanied by such displacement defects in the heating wire. Figure 2(d) reveals a complete absence of signal at the echo of the pipe's inner wall. Concurrently, over-welding has led to displacement and hole defects in the upper heating wire. This incomplete socketing occurs when the pipe's insertion depth is insufficient to cover the heating wire, resulting in an over-welding phenomenon.

The ultrasound phased array technology effectively highlights various defects in the leaky EF joint. Under complex operational conditions, these defects can act as weak points, causing premature failure and significantly reducing the lifespan of PE pipelines.

3.2 Typical service environment factor analysis of polyethylene gas pipe

Although PE has high resistance to acid and alkali, some organic compounds may erode the pipes, causing degradation of pipe performance when PE pipe buried in polluted soil environments for a long time. This degradation can exacerbate the risk of damage to PE pipes due to ground subsidence, urban flooding, urban high-voltage transmission and distribution systems or other factors (Ma, 2018; Ma *et al.*, 2015; Zhu *et al.*, 2018). Figure 3 provides a glimpse into the composition of

Figure 3 Results of physicochemical analysis of the soil in the service environment of P1

Table 1. Characteristic peaks of P1

Peak	Position (time)
1	5.28
2	5.84
3	6.45
4	7.79
5	7.82
6	12.13
7	13.79
8	14.21
9	15.64
10	15.70
11	19.73
12	42.94
13	49.57
14	55.60
15	61.15

Table 2. Organic fraction contained in the soil of P1

Number	Molecular formula	Compound
1	$C_6H_{12}O_2$	Diacetone alcohol
2	$C_6H_{10}O_2$	Hexane-2,4-dione-enol interconjugate isomers
3	$C_6H_{10}O_2$	2,5-Hexanedione
4	C_7H_7Cl	Benzyl chloride
5	$C_8H_{18}O$	2-Ethyl-1-hexanol
6	$C_{14}H_{26}O_2$	4,7-Dihydroxy-2,4,7,9-tetramethyl-5-decyne
7	$C_{14}H_{31}N$	Dodecyl dimethyl tertiary amine
8	$C_{12}H_{27}O_4P$	Tributyl phosphate
9	$C_{15}H_{28}O_4$	Bis(4-methylpent-2-yl) malonate
10	$C_{15}H_{28}O_4$	Bis(4-methylpentan-2-yl) malonate
11	$C_{16}H_{35}N$	N,N-Dimethyl-1-tetradecylamine
12	$C_{22}H_{42}O_6$	Triethylene glycol diisooctanoate
13	$C_{22}H_{42}O_6$	Triethylene glycol diisooctanoate
14	$C_{22}H_{42}O_6$	Triethylene glycol diisooctanoate
15	$C_{24}H_{46}O_7$	Tetraethylene Glycol Diisooctanoate

Note: Table 1 includes the characteristic peaks of P1, and Table 2 shows the organic fraction contained in the soil of P1
Source: Authors' own creation

organic compounds present in the soil surrounding the buried gas leakage section. After identifying the characteristic peaks of these organic compounds, they were calibrated against the library of organic compound characteristic peaks (in Table 1, Figure 3). This analysis of the matching degree allowed for the determination of the specific organic components present in the soil.

As depicted in Tables 1 and 2, Figure 3, the soil samples are abundantly enriched with surfactants, predominantly comprising polyesters, alcohols and amides. Notably, amide compounds exhibit distinct surface-active properties. The presence of these surfactants significantly diminishes the strength of secondary bonds between molecules. This weakening effect reduces the energy barrier for the sliding and disentangling of PE polymer chains, ultimately facilitating the formation of microcavities and stress concentration points. Consequently, the expansion energy required for microdefects to propagate decreases, leading to premature deterioration of the material's mechanical properties.

3.3 Surface microscopic morphology analysis
Figure 4(a) and Figure 4(b) present the micrographs of the exterior surfaces of P1 and P2, respectively. As seen in Figure 4(a), the outer surface of P1 exhibits pronounced exfoliation, debris and microcracks. This exfoliation likely arises from the molecular chain scission resulting from the degradation of PE macromolecules during aging, as suggested by Larché et al. (2012). Furthermore, the presence of surfactants in the soil can decrease the energy barrier for the sliding and disentangling of PE polymer chains, contributing to the formation of micro-voids. Under the combined effects of diminishing mechanical strength and anisotropic internal stresses within the sample, these micro-voids tend to be the origin of microcracks (Rabello and White, 1997; Yang et al., 2008). When the mechanical

Table 1 Characteristic peaks of P1

Peak	Position (time)
1	5.28
2	5.84
3	6.45
4	7.79
5	7.82
6	12.13
7	13.79
8	14.21
9	15.64
10	15.70
11	19.73
12	42.94
13	49.57
14	55.60
15	61.15

Source: Authors' own creation

strength drops below the threshold required to contain internal stresses, minor cracks start to emerge. Conversely, Figure 4(b) reveals that the surface of P2 exhibits minimal defects, primarily consisting of minor scratches that are unavoidable during processing and transportation, maintaining an overall smooth and unblemished appearance.

3.4 Mechanical property
The assessment of mechanical properties holds significant importance in evaluating the performance of PE gas pipe materials. Historically, the calculation of failure analysis for urban pipeline materials based on mechanical principles has

Table 2 Organic fraction contained in the soil of P1

No.	Molecular formula	Compound
1	$C_6H_{12}O_2$	Diacetone alcohol
2	$C_6H_{10}O_2$	Hexane-2,4-dione-enol interconjugate isomers
3	$C_6H_{10}O_2$	2,5-Hexanedione
4	C_7H_7Cl	Benzyl chloride
5	$C_8H_{18}O$	2-Ethyl-1-hexanol
6	$C_{14}H_{26}O_2$	4,7-Dihydroxy-2,4,7,9-tetramethyl-5-decyne
7	$C_{14}H_{31}N$	Dodecyl dimethyl tertiary amine
8	$C_{12}H_{27}O_4P$	Tributyl phosphate
9	$C_{15}H_{28}O_4$	Bis(4-methylpent-2-yl) malonate
10	$C_{15}H_{28}O_4$	Bis(4-methylpentan-2-yl) malonate
11	$C_{16}H_{35}N$	N,N-Dimethyl-1-tetradecylamine
12	$C_{22}H_{42}O_6$	Triethylene glycol diisooctanoate
13	$C_{22}H_{42}O_6$	Triethylene glycol diisooctanoate
14	$C_{22}H_{42}O_6$	Triethylene glycol diisooctanoate
15	$C_{24}H_{46}O_7$	Tetraethylene glycol diisooctanoate

Source: Authors' own creation

Figure 4 Microscopic morphology of the outer surface of (a) P1 and (b) P2, stress–strain curves of (c) P1 and (d) P2 pipe
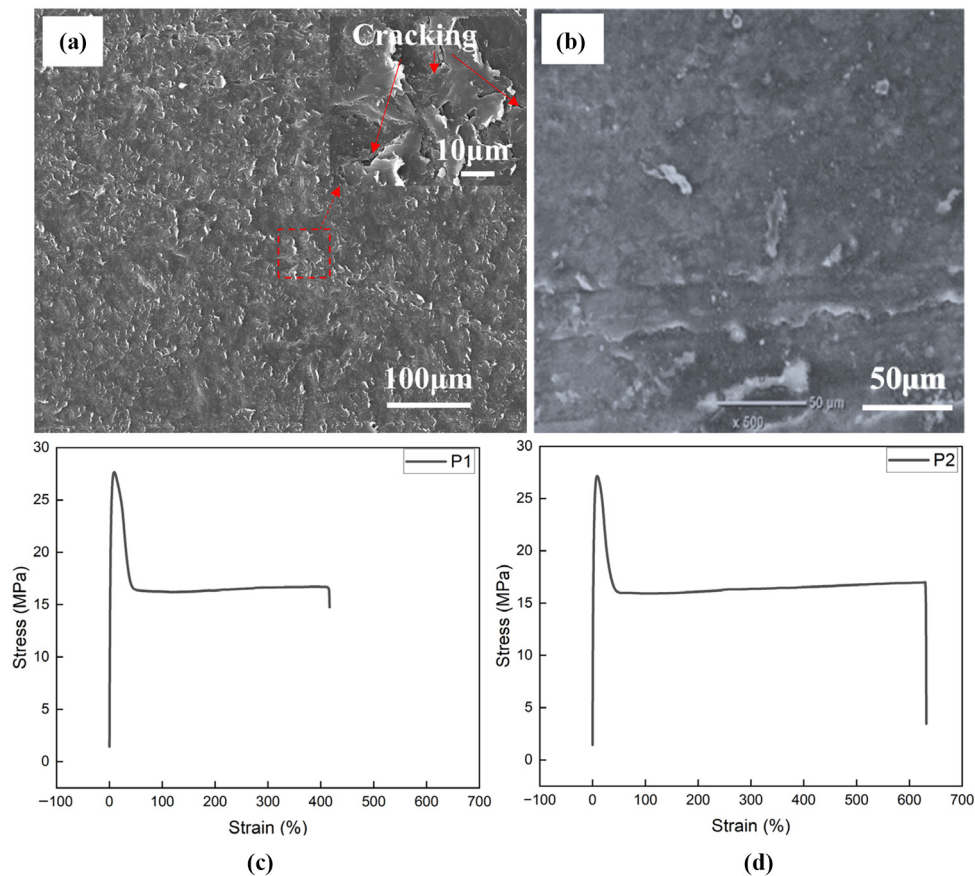
Source: Authors' own creation

been a well-established practice, with the corresponding framework continuously advancing (Guo, 1999; Li, 2012). Figure 4(c) and Figure 4(d) illustrate the stress–strain curves of P1 and P2 pipes, where P1 exhibits a tensile strength of 27.6 MPa and a yield strength of 16.5 MPa, while P2 demonstrates slightly lower values of 27.2 MPa and 16.0 MPa. The differences in these parameters are minimal. According to the specifications outlined in GB 15558.1-2015, it is evident that both P1 (with a break elongation of 413%) and P2 (with a break elongation of 626%) meet the criterion of ≥350%. The

substantial difference in break elongation could potentially be attributed to the premature aging and brittleness of PE pipeline materials in their operational soil environment.

## 3.5 Structural aging performance

The structural aging properties of the outer surface of P1 and P2, as well as the interior surface of P1, were comprehensively analyzed using FTIR, DSC, TG and OIT techniques.

3.5.1 Chemical structure

The FTIR results are depicted in Figure 5, highlighting characteristic peaks that are indicative of PE structure. Specifically, the peaks at $719\,cm^{-1}$, $1,472\,cm^{-1}$ and $2,914\,cm^{-1}$ correspond to the bending vibration of -C-H, the deformation bending of $-CH_2$, and the stretching vibration of -CH, respectively (Zha *et al.*, 2023; Chen *et al.*, 2019). These peaks are features of PE. Moreover, the peaks at $719\,cm^{-1}$ and $1,472\,cm^{-1}$ are attributed to the crystalline phase of PE, and the prominent increase in intensity at $719\,cm^{-1}$ signifies an enhancement in crystallinity, as evident in Figure 5(a).

Notably, on the outer surface of P1 in Figure 5(a), novel peaks emerge at $1,034\,cm^{-1}$, $1,125\,cm^{-1}$, $1,579\,cm^{-1}$ and $1,541\,cm^{-1}$. These changes are likely associated with chain scission and crosslinking reactions on the P1 surface. Short chains may participate in crosslinking reactions or bond with oxygen radicals to form ether groups (-C-O-C, within the range of $1,000\,cm^{-1}$ to $1,200\,cm^{-1}$) (Hu *et al.*, 2018; Colom *et al.*, 2003) and carbonyl groups (C = O, within the range of $1,540\,cm^{-1}$ to $1,600\,cm^{-1}$). Furthermore, surfactants present in the soil environment, such as ketones, carboxylic acids, peroxides and esters, can adhere to the pipe surface, resulting in additional peak formation and accelerating the aging process of PE pipe materials. It is crucial to note that these substances have not yet penetrated the interior of P1 [(as seen in Figure 5(b)]; thus, its FTIR spectrum remains similar to P2 [depicted in Figure 5(c)]. As aging progresses, the degree of chain breakage and degradation in PE pipes gradually increases, potentially leading to a decrease in thermal stability.

Figure 5 FTIR spectrogram
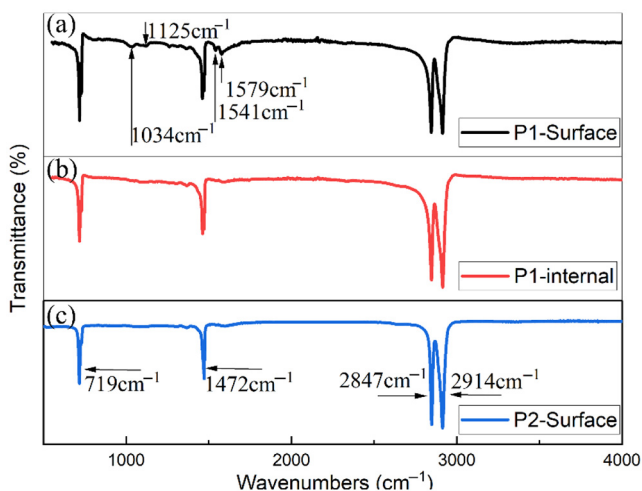
Source: Authors' own creation

### 3.5.2 Melt-transition temperature and crystallinity

Crystallinity refers to the proportion of crystalline area in a polymer, which reflects the regularity of the internal structure of the material. High crystallinity indicates great impact strength but poor ductility. The DSC curves of P1 and P2 are shown in Figure 6(a)–Figure 6(c).

From the DSC curves in Figure 6, we can obtain the melting temperature (T_{eim}) and peak temperature (T_{pm}), and calculate the crystallinity of the material, as shown in Figure 6(d). It can be seen that there is a small difference in the melting temperature between the outer surface of P1 and P2, but the melting temperature of the outer surface of P1 is lower than that of its interior layer. The crystallinity of P1 is slightly higher than that of P2. Generally, during the initial aging stage of polymer pipes, crystallinity increases significantly, and there is a strong intermolecular force. During aging, large molecular chains break down into small molecular chains, which are prone to secondary crystallization in amorphous regions. This process results in an increase in crystallinity, in line with FTIR results. When the structural aging is intensified, oxygen can enter the interior of the sample through the grooves to accelerate the oxidation of the amorphous regions, generating oxygen-containing functional groups and leading to a decrease in crystallinity. Therefore, P1 undergoes secondary crystallization under the influence of soil ambient temperature with intense activity of amorphous structural chain segments. However, these processes tend to occur at localized area, leading to a structural heterogeneity. Consequently, cracks can develop at the interface between the brittle and soft phases. Prolonged exposure of the pipe to surfactants in a polluted soil environment is likely to expedite the rate of crack initiation on the PE pipe surface, particularly if the pipe is in long-term service (Zhang *et al.*, 2022). As a result, the service mechanical properties and safety of PE pipes are greatly reduced.

3.5.3 Thermal weight loss

The thermal decomposition behavior of PE pipes is shown in Figure 7(a)–Figure 7(c). As the thermal decomposition temperature increases, the weight of PE pipes decreases continuously. The thermal decomposition behavior of PE pipes at different locations varies. P1 and P2 have the maximal rate of thermal degradation between 400 and 500°C. And, the final mass loss of P1 and P2 reaches more than 97%. It can be seen that all TG plots are similar to each other and have only one platform, indicating that the thermal degradation of buried PE gas pipes during service is a one-step process (Huo *et al.*, 2013; Xu *et al.*, 2010), which is related to random chain scission and free radical formation.

Generally, the thermal degradation reaction of PE is a random chain scission reaction, which can be divided into three processes. In the early stage of degradation, as the temperature rises to the melting temperature, the polymer melts and its relative molecular mass decreases, but the polymer mass remains basically unchanged. In the middle stage, the large molecular chain breaks into a large number of small molecular chains. And, the volatilization of small molecular chains contributes to a sharp decrease of polymer mass. In the late stage, the polymer completely carbonizes, and the residue mass remains unchanged (Xin *et al.*, 2016; Liu *et al.*, 2015). Figure 7(d) displays the characteristic temperature of thermal decomposition of PE pipe. It can be seen that the characteristic

Figure 6 (a), (b), (c) DSC results of P1-Surface, P1-Internal and P2-Surface, (d) Transition temperature and crystallinity of service pipe
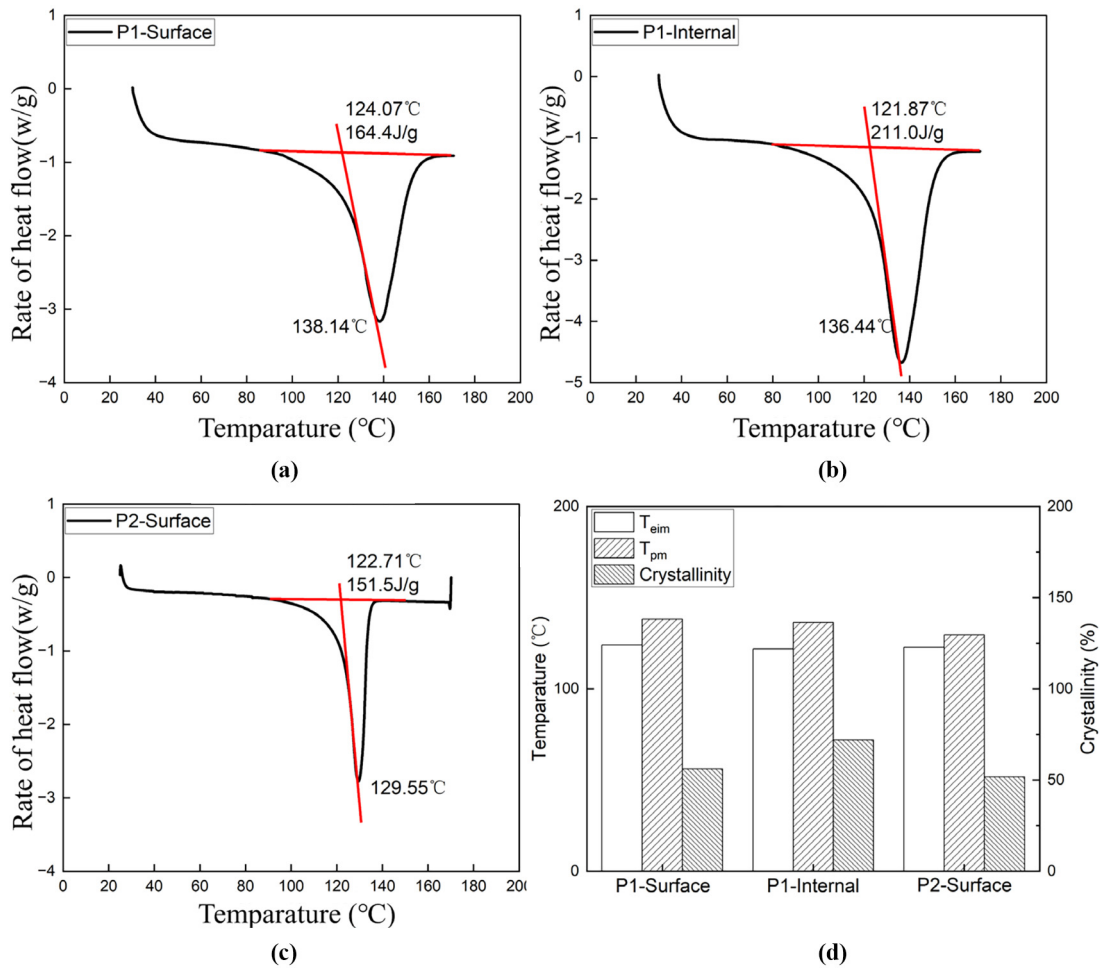
Source: Authors' own creation

thermal decomposition temperature of P1 increases with the extension of aging time, indicating that aging has an impact on the maximum thermal decomposition temperature of PE. This may be related to the increase of crystallinity of P1, which leads to more regular segments of PE polymer and increases the energy required for material decomposition. In addition, fewer amorphous segments that are easier melting decomposition cause further increases of the decomposition temperature.

3.5.4 Oxidation induction time
During service, oxygen and corrosive substances in the environment will react chemically with PE pipes. Anti-oxidants are beneficial to delay this degradation process, generally by capturing free radicals during the reaction process. OIT test is an effective method for evaluating the degree of polymer degradation. It can characterize the thermal stability of polymers and reflect the consumption of antioxidants. OIT can be measured quickly and easily using DSC (Wu *et al.*, 2019). Through OIT test, it is possible to evaluate the thermal oxidative stability of polyolefins simply and quickly, providing an effective analytical method for performance evaluation in the research and development process of polyolefin products

(Archodoulaki *et al.*, 2006). The OIT results are shown in Figure 8(a) and Figure 8(b).

Figure 8(c) shows that the OIT of P1 was significantly higher than that of P2 (100 min, much larger than 24.82 min). The outer surface groups of PE pipe were stimulated by the surfactants and oxidized rapidly, generating a large number of free radicals, which weakened the antioxidant capacity and thermo-oxidative stability of PE pipe. At the same time, oxygen penetrates into the interior of the pipe through surface defects and consumes a large amount of antioxidants. Pipe degradation becomes dominant (Miao *et al.*, 2017). Thus, the antioxidant properties of both the interior and outer surface of the pipe deteriorate.

3.6 Influence of surfactants on aging behavior of polyethylene pipe

Although the excellent performance of PE gas pipes makes them have a very wide application prospect in gas engineering, there are still many potential safety hazards in specific use environments. This is because the characteristics of PE polymer chains determine that they will suffer structural deterioration in extreme environments such as exposure to heat

Figure 7 TG curves of (a), (b) P1 and (c) P2, (d) transition temperature and crystallinity of service pipe
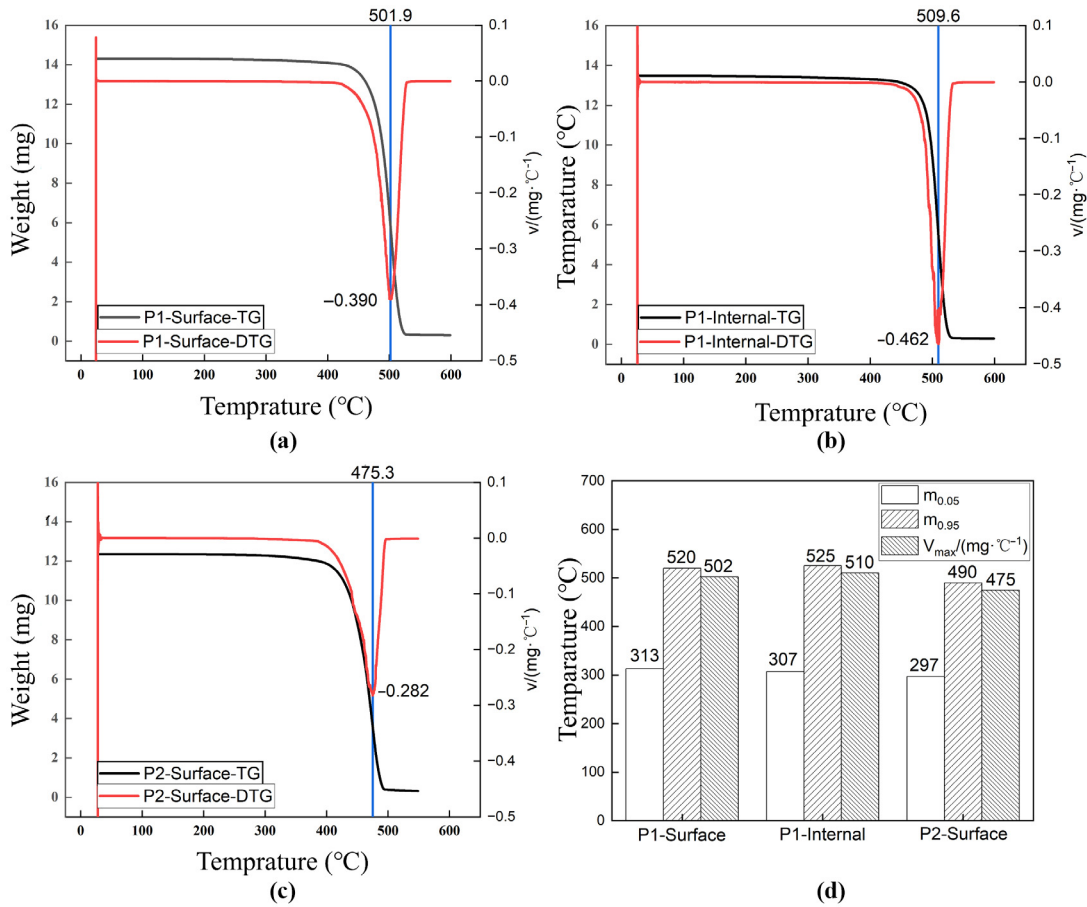
Source: Authors' own creation

Figure 8 (a, b) OIT test of P1-Surface and P1-Internal, respectively, (c) OIT results
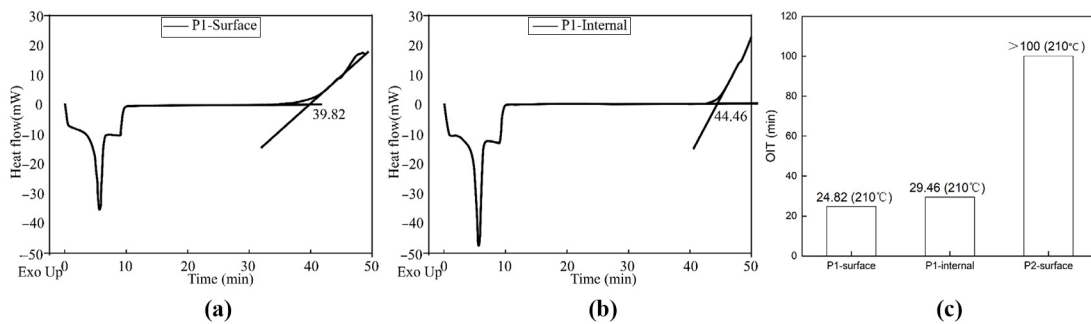
Source: Authors' own creation

and moisture, and organic chemical media erosion. Due to the lack of polar bonds and its high hydrophobicity, PE has high resistance to biological and chemical erosion (Mukherjee *et al.*, 2018). However, PE is prone to thermal oxygen aging in the amorphous region, forming carbonyl, ether and other polar groups, which become the attack sites of surfactants (C_7H_7Cl, $C_{14}H_{31}N$, etc.). The long hydrocarbon chain of PE breaks at the polar group, forming small molecular chain segments, which leads to the formation of microcracks on the surface of

PE pipes [Figure 4(a)] (Mukherjee *et al.*, 2018; Pandey and Singh, 2001). Meanwhile, due to its amphiphilic properties, surfactants can also invade the crystalline region of PE, causing lattice swelling and promoting oxygen diffusion (Mukherjee *et al.*, 2018). At the same time, the binding strength of the chain segments in these regions decreases, further accelerating the oxidation and chain scission of the crystalline region. Oxidation in the amorphous region may release the microcrystalline particles, resulting in an increase in crystallinity [Figure 6(d)]

([Manzur *et al.*, 2004](#)). In particular, connecting fittings such as EF joint have weak resistance to the environmental effects, making them vulnerable parts of PE pipes. The PE molecular chain segments in the cold fusion area of EF joint are more prone to thermal oxygen aging. If surface oxidants diffuse into these regions, the chain breaking of PE molecules in this region will be accelerated, leading to reduced strength and stress concentration. The defective position of EF joint is more likely to crack and lead to gas leakage. Therefore, it is necessary to pay close attention to the performance of PE gas pipes in the soil environment to avoid major safety hazards.

4. Conclusion

An PE gas pipeline in Beijing is failed after only five years' service due to gas leakage at EF joint. To find out whether the failure of PE pipeline is related to the role of service environment, combined with the results of physical and chemical analysis of soil, the microscopic morphology and chemical structure of the leakage pipe was analyzed:

- The ultrasonic phased array spectra showed that cold fusion occurred inside the EF joint, forming defects such as holes and misaligned heating wires.
- The strength of the failed pipe was high enough, but the toughness was greatly reduced.
- The outer surface layer of the failed pipe undergoes thermo-oxidative aging and forms -C-O-, with a significant decrease in OIT and an increase in thermal decomposition temperature.
- The soil near the failure site contains many surfactants. Under the catalytic effect of surfactants, the polymer chain segments of PE pipe break into small molecules. Therefore, pore defects produce, resulting in an acceleration of crack nucleation. Additionally, this process can also impact the defects present in EF joint, thereby increasing the risk of gas leakage at EF joint.

References

Archodoulaki, V.M., Lüftl, S. and Seidler, S. (2006), "Oxidation induction time studies on the thermal degradation behaviour of polyoxymethylene", *Polymer Testing*, Vol. 25 No. 1, pp. 83-90, doi: 10.1016/j.polymertesting.2005.08.011.

Bredács, M., Frank, A., Bastero, A., Stolarz, A. and Pinter, G. (2018), "Accelerated aging of polyethylene pipe grades in aqueous chlorine dioxide at constant concentration", *Polymer Degradation and Stability*, Vol. 157, pp. 80-89.

Caravaca, D.S., Bird, C. and Kleiner, D. (2007), "Ultrasonic phased array inspection of electrofusion joints in polyethylene pipes", *Insight – Non-Destructive Testing and Condition Monitoring*, Vol. 49 No. 2, pp. 83-86, doi: 10.1784/INSI.2007.49.2.83.

Chen, G., Yang, Y., Zhou, C., Zhou, Z. and Yan, D. (2019), "Thermal-oxidative aging performance and life prediction of polyethylene pipe under cyclic and constant internal pressure", *Journal of Applied Polymer Science*, Vol. 136 No. 28, p. 47766.

Colom, X., Canavate, J., Sunol, J.J., Pages, P., Saurina, J. and Carrasco, F. (2003), "Natural and artificial aging of polypropylene–polyethylene copolymers", *Journal of Applied Polymer Science*, Vol. 87 No. 10, pp. 1685-1692.

Egerton, J.S., Lowe, M.J.S., Huthwaite, P. and Halai, H.V. (2017), "Ultrasonic attenuation and phase velocity of high-density polyethylene pipe material", *The Journal of the Acoustical Society of America*, Vol. 141 No. 3, pp. 1535-1545, doi: 10.1121/1.4976689.

Frederick, C., Porter, A. and Zimmerman, D. (2010), "High-density polyethylene piping butt-fusion joint examination using ultrasonic phased array", *Journal of Pressure Vessel Technology*, Vol. 132 No. 5, doi: 10.1115/1.4001212.

Grabmayer, K., Wallner, G.M., Beißmann, S., Braun, U., Steffen, R., Nitsche, D., Röder, B., Buchberger, W. and Lang, R.W. (2014), "Accelerated aging of polyethylene materials at high oxygen pressure characterized by photoluminescence spectroscopy and established aging characterization methods", *Polymer Degradation and Stability*, Vol. 109, pp. 40-49.

Guo, Q. (1999), "Thermal aging test and life evaluation of low voltage x LPE cable", *Wire and Cable*, No. 2, pp. 42-48.

Hoàng, E.M. and Lowe, D. (2008), "Lifetime prediction of a blue PE100 water pipe", *Polymer Degradation and Stability*, Vol. 93 No. 8, pp. 1496-1503, doi: 10.1016/j.polymdegradstab.2008.05.008.

Hu, W.X., Liu, C.Q., Liu, W.J. and Ren, X.C. (2018), "The study on the stress and photo-oxidative aging of polyethylene cable sheath under different processing conditions", *Macromolecular Research*, Vol. 26 No. 5, pp. 426-437, doi: 10.1007/s13233-018-6052-9.

Huo, R.M., Liu, F. and Jiang, P.K. (2013), "TG rapid evaluation method research of thermal life of cross-linked polyethylene", *Insulating Materials*, Vol. 46 No. 6, pp. 19-24, doi: 10.16790/j.cnki.1009-9239.im.2013.06.006.

Larché, J.F., Bussière, P.O., Therias, S. and Gardette, J.L. (2012), "Photooxidation of polymers: relating material properties to chemical changes", *Polymer Degradation and Stability*, Vol. 97 No. 1, pp. 25-34, doi: 10.1016/j.polymdegradstab.2011.10.020.

Leskovics, K., Kollár, M. and Bárczy, P. (2006), "A study of structure and mechanical properties of welded joints in polyethylene pipes", *Materials Science and Engineering: A*, Vol. 419 Nos 1/2, pp. 138-143, doi: 10.1016/j.msea.2005.12.019.

Li, M.Y. (2012), "Experimental study and mechanical analysis of buried polyethylene gas pipe", *China Special Equipment Safety*, Vol. 28 No. 3, pp. 15-19.

Li, X.L. and Chen, F.Y. (1998), "Polyethylene (PE) pipes fitting for used in city gas system", *Pipeline Technique and Equipment*, No. 6, pp. 34-36.

Li, Q., Lu, Q., Chen, Y.C., Su, J.W. and Yang, J. (2023), "Effect of the ultrasonic phased array on defect detection of HDPE electro-fusion joint", *Journal of Physics: Conference Series*, Vol. 2419 No. 1, doi: 10.1088/1742-6596/2419/1/012070.

Li, M.D., Chen, G.H., Yang, B., Yang, Y., Huang, X.Z. and Huang, G.G. (2019), "Effect of heat aging on the performance of PE pipe under constant internal pressure", *Plastics*, Vol. 48 No. 2, pp. 127-131.

Liu, Y.F., Chen, G., Chen, L., Luo, Z., He, M. and Liu, Y. (2015), "Research on thermal degradation of silane naturally cross-linked polyethylene", *Chemical Propellants & Polymeric Materials*, Vol. 13 No. 5, pp. 84-87, doi: 10.16572/j.issn1672-2191.201505019.

Ma, Z.Y. (2018), "Discussion on the influence of buried depth on gas pipeline leakage and emergency repair", *Urban Construction Theory Research (Electronic Edition)*, No. 10, p. 80.

Ma, G.Y., Wang, X., Li, D., Liu, B.B. and Huang, T.L. (2015), "Influence of burial depth on natural gas pipeline leakage in flat area", *Journal of Southwest Petroleum University (Science & Technology Edition)*, Vol. 37 No. 2, pp. 165-172.

Manzur, A., Limón-González, M. and Favela-Torres, E. (2004), "Biodegradation of physicochemically treated LDPE by a consortium of filamentous fungi", *Journal of Applied Polymer Science*, Vol. 92 No. 1, pp. 265-271.

Matthew, S.P., Kayte, M.D., Traci, L.M., Richard, E.J., Trenton, S.H., Susan, L.C., Royce, M., Kevin, J.N. and Anthony, D.C. (2016), "Evaluation of ultrasonic phased-array for detection of planar flaws in high-density polyethylene (HDPE) butt-fusion joints", *Proceedings of the ASME 2016 Pressure Vessels and Piping Conference*, Vol. 6B, doi: 10.1115/PVP2016-63688.

Mei, S. (2004), "On the present situation and prospect of the application of PE pipe", *Journal of Guangzhou University (Natural Science Edition)*, No. 3, pp. 276-280.

Miao, X.P., Kang, P., Guo, R.H. and Zhe, D.M. (2017), "Isothermal oxidation induction time of high density polyethylene/low density polyethylene blends", *Petrochemical Industry*, Vol. 46 No. 12, pp. 1479-1482.

Mukherjee, S., RoyChaudhuri, U. and Kundu, P.P. (2018), "Biodegradation of polyethylene via complete solubilization by the action of Pseudomonas fluorescens, biosurfactant produced by Bacillus licheniformis and anionic surfactant", *Journal of Chemical Technology & Biotechnology*, Vol. 93 No. 5, pp. 1300-1311.

Pandey, J.K. and Singh, R.P. (2001), "UV-irradiated biodegradability of ethylene– propylene copolymers, LDPE, and I-PP in composting and culture environments", *Biomacromolecules*, Vol. 2 No. 3, pp. 880-885.

Rabello, M.S. and White, J.R. (1997), "The role of physical structure and morphology in the photodegradation behaviour of polypropylene", *Polymer Degradation and Stability*, Vol. 56 No. 1, pp. 55-73.

Shapheek, M. and Shrivastava, N. (2020), "Optimization of cooling time for polyethylene fusion joints", *Materials Today: Proceedings*, Vol. 28, pp. 1267-1272, doi: 10.1016/j.matpr.2020.04.152.

Shin, H.J., Jang, Y.H. and Kwan, J.R. (2003), "Ultrasonic array approach for the evaluation of electrofusion joints of polyethylene gas pipe", *American Institute of Physics*, Vol. 657 No. 1, pp. 659-665.

Tao, Y., Shi, J., Guo, W. and Zheng, J. (2023), "Convolutional neural network based defect recognition model for phased array ultrasonic testing images of electrofusion joints", *Journal of Pressure Vessel Technology*, Vol. 145 No. 2, p. 024502.

Wang, J. and Peng, J. (2005), "Structural and mechanical properties of PE-HD in aging test", *China Plastics*, Vol. 1, pp. 46-49.

Wang, W.W., Rong, H. and Zou, M.Z. (2000), "Trenchless techniques to lay polyethylene pipe", *Gas & Heat*, No. 2, pp. 32-34.

Wang, Y., Lan, H.Q. and Meng, T. (2019), "Lifetime prediction of natural gas polyethylene pipes with internal pressures", *Engineering Failure Analysis*, Vol. 95, pp. 154-163.

Weon, J.I. (2010), "Effects of thermal ageing on mechanical and thermal behaviors of linear low density polyethylene pipe", *Polymer Degradation and Stability*, Vol. 95 No. 1, pp. 14-20, doi: 10.1016/j.polymdegradstab.2009.10.016.

Wu, B., Cheng, W. and Wen, H.Y. (2019), "Effect of oxidation induction time on thermal oxygen aging characteristics of high density polyethylene", *China Plastics*, Vol. 33 No. 4, pp. 22-25+88.

Xin, W., Zhang, F.G., Yuan, J., Tang, X.X. and Zhang, L. (2016), "Kinetics of thermal degradation of recycled high- density polyethylene", *Shandong Chemical Industry*, Vol. 45 No. 7, pp. 37-41, doi: 10.19319/j.cnki.issn.1008-021x.2016.07.015.

Xiong, Z.M., Sun, J.W., Wu, Z.J. and Chen, M.J. (2011), "Study on slow crack growth properties of polyethylene pipe and the corresponding evaluation methods", *China Plastics Industry*, Vol. 39 No. 8, pp. 10-14.

Xiong, Z.M., Wu, Z.J., Hua, Y., Wei, R.Q. and Zhe, D.M. (2016), "Study on accelerated testing of slow crack growth resistance of high density polyethylene pipe", *China Synthetic Resin and Plastics*, Vol. 33 No. 4, pp. 60-63.

Xu, L., Wu, W.J. and Ding, Y.Y. (2010), "Investigation on thermal degradation behavior of typical thermoplastics polymer", *Fire Safety Science*, Vol. 19 No. 3, pp. 143-149.

Yang, R., Liu, Y. and Yu, J. (2008), "Spatial heterogeneity of photo-oxidation and its relation with crack propagation in polyethylene composites", *Polymer Engineering & Science*, Vol. 48 No. 11, pp. 2270-2276.

Zhang, C.Q., Li, C., Zhan, C.M., Wang, P.Z. and Gao, J. (2022), "Study on the causes of failure in the case of ablation and failure of polyethylene gas pipes and structural performance degradation of heat-affected zone", *Hans Journal of Chemical Engineering and Technology*, Vol. 12, p. 399.

Zha, S., Lan, H.Q. and Huang, H. (2022), "Review on lifetime predictions of polyethylene pipes: limitations and trends", *International Journal of Pressure Vessels and Piping*, Vol. 198, p. 104663.

Zha, S., Lan, H.Q., Lin, N. and Meng, T. (2023), "Degradation and characterization methods for polyethylene gas pipes after natural and accelerated aging", *Polymer Degradation and Stability*, Vol. 208.

Zheng, J.Y., Shi, J.F. and Guo, W.C. (2012), "Development of nondestructive test and safety assessment of electrofusion joints for connecting polyethylene pipes", *Journal of Pressure Vessel Technology*, Vol. 134 No. 2, doi: 10.1115/1.4004869.

Zhu, Q.J., Zhao, C., Chen, Y.H., Li, X. and Yin, X. (2018), "Influence factors and protection measures of buried natural gas pipeline leakage", *Chinese Journal of Environmental Engineering*, Vol. 12 No. 2, pp. 417-420.

Corresponding author

Qing Bao can be contacted at: bjrq_baoqing@163.com